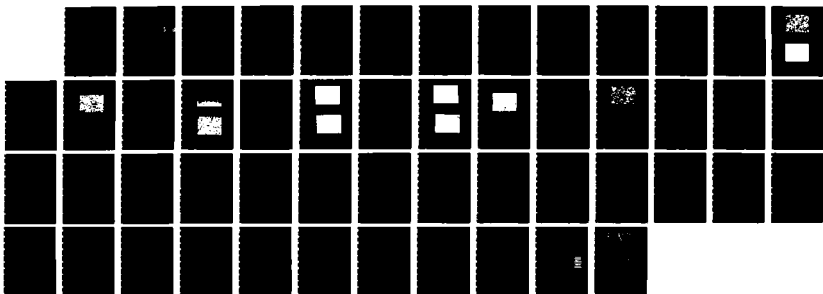


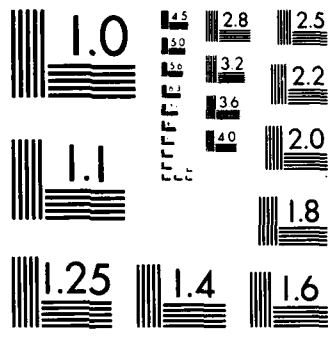
AD-A184 500

ULTRA-FINE GRAINED ALLOY MATERIAL (U) JOHNS HOPKINS UNIV 1/1
BALTIMORE MD J D CLARK ET AL JUN 87 BRL-CR-573

UNCLASSIFIED

F/G 11/6 1 NL





MICROCOPY RESOLUTION TEST CHART
NATIONAL BUREAU OF STANDARDS-1963-A

AD

12

AD-A184 500

CONTRACT REPORT BRL-CR-573

DTIC
ELECTE
SEP 14 1987
S D

ULTRA- FINE GRAINED
ALLOY MATERIAL

JOHNS HOPKINS UNIVERSITY
34TH AND CHARLES STREETS
BALTIMORE, MARYLAND 21218

JUNE 1987

APPROVED FOR PUBLIC RELEASE; DISTRIBUTION UNLIMITED

US ARMY BALLISTIC RESEARCH LABORATORY
ABERDEEN PROVING GROUND, MARYLAND

Destroy this report when it is no longer needed.
Do not return it to the originator.

Additional copies of this report may be obtained
from the National Technical Information Service,
U. S. Department of Commerce, Springfield, Virginia
22161.

The findings in this report are not to be construed as an official
Department of the Army position, unless so designated by other
authorized documents.

The use of trade names or manufacturers' names in this report
does not constitute indorsement of any commercial product.

UNCLASSIFIED

SECURITY CLASSIFICATION OF THIS PAGE

REPORT DOCUMENTATION PAGE

Form Approved
OMB No 0704-0188
Exp Date Jun 30, 1986

1a. REPORT SECURITY CLASSIFICATION Unclassified		1b. RESTRICTIVE MARKINGS	
2a. SECURITY CLASSIFICATION AUTHORITY		3. DISTRIBUTION / AVAILABILITY OF REPORT	
2b. DECLASSIFICATION / DOWNGRADING SCHEDULE			
4. PERFORMING ORGANIZATION REPORT NUMBER(S)		5. MONITORING ORGANIZATION REPORT NUMBER(S)	
6a. NAME OF PERFORMING ORGANIZATION The Johns Hopkins University	6b. OFFICE SYMBOL (if applicable)	7a. NAME OF MONITORING ORGANIZATION Ballistic Research Laboratory	
6c. ADDRESS (City, State, and ZIP Code) 34th and Charles Streets Baltimore, MD 21218		7b. ADDRESS (City, State, and ZIP Code) Aberdeen Proving Ground, MD 21005-5066	
8a. NAME OF FUNDING / SPONSORING ORGANIZATION Ballistic Research Laborator	8b. OFFICE SYMBOL (if applicable) SLCBR-TB-S	9. PROCUREMENT INSTRUMENT IDENTIFICATION NUMBER	
8c. ADDRESS (City, State, and ZIP Code) Aberdeen Proving Ground, MD 21005-5066		10. SOURCE OF FUNDING NUMBERS	
		PROGRAM ELEMENT NO.	PROJECT NO.
		TASK NO.	WORK UNIT ACCESSION NO.
11. TITLE (Include Security Classification) Ultra-Fine Grained Alloy Material			
12. PERSONAL AUTHOR(S) James B. Clark and Paul Kelley			
13a. TYPE OF REPORT Contractor Report	13b. TIME COVERED FROM _____ TO _____	14. DATE OF REPORT (Year, Month, Day)	15. PAGE COUNT
16. SUPPLEMENTARY NOTATION			
17. COSATI CODES		18. SUBJECT TERMS (Continue on reverse if necessary and identify by block number)	
FIELD	GROUP	Ultrafine Grain Grain Boundaries Microstructure	
		Amorphous Eutectic	
		Thermomechanical Alloys	
19. ABSTRACT (Continue on reverse if necessary and identify by block number)			
Thermomechanical processing has been applied to selected alloys to produce enhanced ductility. A fine-grained microstructure at high ductility was produced in eutectic lead-tin and lead-antimony.			
Melt-extracted fibers of lead-antimony were also produced and exhibited high ductility.			
Microstructural analyses were performed using optical and X-ray methods. It was concluded that ductility enhancement was due to the presence of large quantities of metastable, disordered grain boundary material.			
20. DISTRIBUTION / AVAILABILITY OF ABSTRACT <input type="checkbox"/> UNCLASSIFIED/UNLIMITED <input checked="" type="checkbox"/> SAME AS RPT <input type="checkbox"/> DTIC USERS		21. ABSTRACT SECURITY CLASSIFICATION Unclassified	
22a. NAME OF RESPONSIBLE INDIVIDUAL P. W. Kingman		22b. TELEPHONE (Include Area Code) (301) 278-6878	22c. OFFICE SYMBOL SLCBR-TB-A

DD FORM 1473, 84 MAR

83 APR edition may be used until exhausted
All other editions are obsolete

SECURITY CLASSIFICATION OF THIS PAGE

UNCLASSIFIED

TABLE OF CONTENTS

	<u>Page</u>
LIST OF FIGURES	iii
LIST OF TABLES	v
I. INTRODUCTION	1
II. THERMOMECHANICAL PROCESSING TECHNIQUES	4
A. Eutectic Lead-Tin.	4
B. Aluminum Bronze.	6
C. Eutectic Lead-Antimony	10
III. TENSILE TESTING OF SUPERPLASTIC ALLOYS	15
IV. ZINC AND ZINC ALLOYS RESULTS	21
V. X-RAY POLE FIGURES	24
VI. DENSITY MEASUREMENTS	28
VII. SUMMARY.	34
VIII. RECOMMENDATIONS FOR FUTURE WORK.	37
REFERENCES	39
DISTRIBUTION LIST.	41

Accession For	
NTIS CRA&I	<input checked="" type="checkbox"/>
DTIC TAB	<input type="checkbox"/>
Unannounced	<input type="checkbox"/>
Justification	
By _____	
Date/Date of _____	
Availability Codes	
Avail and/or _____	
Unannounced _____	
A-1	

LIST OF FIGURES

<u>Fig. No.</u>		<u>Page</u>
1	Microstructure of Lead-Tin as Cast	5
2	Microstructure of Lead-Tin, 95% Reduction.	5
3	Microstructure of Lead-Tin 95% Reduction and Heat Treated at 160°C	7
4	Aluminum-Copper Phase Diagram.	8
5	Microstructure of Aluminum-Bronze as Cast.	9
6	Microstructure of Aluminum-Bronze 95% Reduction and Annealed	9
7	Microstructure of Lead-Antimony as Cast.	11
8	Microstructure of Lead-Antimony, 94% Reduction	11
9	Microstructure of Lead-Antimony Moss	13
10	Microstructure of Lead-Antimony Fibers	13
11	Microstructure of Lead-Antimony Stir-Cast.	14
12	Microstructure of Lead-Antimony 97% Reduction.	16
13	Elongation vs. Annealing Time for Eutectic Lead-Tin.	18
14	Hardness vs. Annealing Time for Lead-Tin	19
15	Hardness vs. Annealing Time at Room Temperature for Lead-Tin	20
16	Variation in the X-ray Peak Area Divided by Total Area vs. Percent Reduction for Pure Zinc.	29
17	Variation in the X-ray Peak Area Divided by Total Area vs. Percent Reduction for Zinc with 88ppm Copper	30
18	Variation in Density with Cold Rolling, Pure Zinc.	30
19	Variation in Density with Cold Rolling, Zinc - 88ppm Copper	32
20	Hardness-Distance Profile, Pure Zinc	32

<u>Fig. No.</u>		<u>Page</u>
21	Hardness-Distance Profile, Zinc - 88ppm Copper	33
22	Hardness-Distance Profile After Cold Rolling, Pure Zinc. . .	33
23	Hardness-Distance Profile After Cold Rolling, Zinc - 88ppm Copper	35

LIST OF TABLES

<u>Table No.</u>	<u>Page</u>
I. Heat Treatment of Lead-Tin.	16
II. Elongation of Lead-Antimony Alloys at Room Temperature. . . .	22
III. Angular Dispersive Results for Pure Zinc.	22
IV. Angular Dispersive Results for Zinc-Copper.	23
V. Pure Zinc Diffractometer Measurements	23
VI. Values of the Integrated Areas Under the $(10\bar{1}1)$ Pole Figure Trace for Pure Zinc (99.9% Pure).	27
VII. Values of the Integrated Areas Under the $(10\bar{1}1)$ Pole Figure Trace for Zinc/Copper	29

Ultra-Fine Grained Alloy Material

Introduction

Suitable thermomechanical processing schedules have been developed to obtain a fine grain size in eutectic lead-antimony (Pb-Sb), aluminum bronze (Cu-10-11%Al-3% Fe) and in eutectic lead-tin (Pb-Sn). A stable fine grain size on the order of 1-10 microns, a testing temperature of greater than one half the absolute melting point and a strain rate sensitivity factor (m) of greater than 0.3 are usually required to see superplastic behavior in certain alloys. Lead-tin was one of the first alloys in which superplastic behavior was observed. C.E. Pearson showed that the ductility was greatly enhanced in an extruded lead-tin alloy in 1934 (1). Constant strain rate tests of 50 percent per minute conducted 1/2 hour after the rods were extruded showed that the lead-tin had a possible elongation of 1122 percent. If the extruded rods were stored for 70 days, only 25 percent elongation was possible. C.E. Pearson also observed that the deformation was by viscous flow at the grain boundaries. More recently Ahmed and Langdon tested a sample of 6.9 micron grain size lead-tin at 413°K and at a strain rate of $1.33 \times 10^{-4} \text{ sec}^{-1}$ and measured an elongation of 4850 percent without failure (2). This eutectic lead-tin was cast and rolled to the final thickness of 0.254 cm at room temperature.

Most of the fine grained superplastic alloys are either eutectic or eutectoid alloys with two or more phases which act to prevent grain growth at the testing temperatures. The main structural criteria requires the structure to have a stable fine grain size on the order of 1 to 10 microns. Associated with this fine grain size is the large volume of material near the grain boundaries. This volume of interface material could serve as a sink for dislocations and vacancies so the grain material would become softer and grain boundary sliding would be easier. It should be possible to develop this high entropy grain boundary structure by either mechanical or thermomechanical processing.

To understand the processing necessary to obtain the high entropy grain boundary structure, pure zinc was rolled and the percentage of crystalline material measured using x-ray diffraction. Commercial purity zinc was shown to be superplastic after a 90 percent rolling reduction by Naziri and Pearce (3). They observed that a 200 percent elongation was possible when the zinc was tested at a crosshead speed of 0.002 in/min. The freshly rolled zinc was ductile but it tended to harden after 4 days. Alloying elements of lead, cadmium and iron were added to stabilize the fine grain size and retain the enhanced ductility. Aust et al. showed in 1968 that when elements with K , the equilibrium distribution coefficient, of greater than 1 were added, the grain boundary region was softened (4). When 100 ppm. of gold was added to the zinc, a soft region on the order of 80 microns wide formed in the vicinity of the grain boundary. If this soft grain boundary region remained when the zinc was

rolled, this would account for a large volume of soft material. This soft material would enhance grain boundary sliding and accommodation.

One method of measuring the volume of high entropy or disordered material at the grain boundaries is by x-ray analysis. Angela Rosasco at The Johns Hopkins University showed that it was possible to follow the degree of crystallinity in a Metglass ribbon by using energy dispersive x-ray diffraction and by looking at the intensity of the crystalline peaks to determine if the material was crystalline (5). Amorphous ribbons had an almost flat intensity versus diffraction angle spectrum while the crystalline ribbons had sharp (intense) crystalline peaks.

In rolling the pure zinc, a strong rolling texture developed which caused the intensity of certain peaks to increase and other peaks to decrease. To avoid the influence of the preferred orientation in the angular dispersive x-ray results, a single plane was chosen and the Siemens Texture Diffractometer was used to obtain x-ray pole figures. The pole figures showed the development of a rolling texture in zinc where the basal planes are tilted 35 to 45 degrees toward the rolling direction. The area under the texture spectrum was integrated. The area under the crystalline peaks was measured and compared to the total area under the spectrum. By dividing the peak area to the total area, it was possible to obtain a relative measure of the volume percent of crystalline material. The degree of crystallinity was measured as a function of thermomechanical processing in pure zinc and zinc with 88 ppm. of copper.

Thermomechanical Processing Techniques

Eutectic Lead-Tin

Eutectic lead-tin (61.9 percent tin and 38.1 percent lead) was obtained by melting Straits tin (99.8% pure) and St. Joseph lead (99.9% pure) in a plumbago crucible and casting it into an iron mold. The iron mold was coated with Aquadag graphite emulsion to prevent contamination. These 1 inch thick castings were allowed to air cool to room temperature and samples were obtained for microstructural characterization. These samples were polished and etched with 8 parts glycerol, 1 part acetic acid and 1 part nitric acid at a temperature of 40°C. Figure 1 shows the coarse as-cast structure of the eutectic lead-tin. The 1 inch thick castings were rolled at room temperature to a 95 percent reduction using a reduction in thickness of 0.050 inch per pass. At a 95 percent reduction, the sheets were tensile tested and seen to be extremely ductile. The microstructure after rolling is shown in Figure 2. This microstructure consists of two phases α (lead-rich) and β (tin-rich) which are present at room temperature. The light phase is the tin rich phase and the dark phase is the lead rich phase. This rolled lead-tin had a mean linear intercept length of 3.6 microns. Sheets of this fine grained rolled lead-tin were provided to Aberdeen Proving Ground for further testing. An additional 837 square inches of eutectic lead-tin was processed as described above, but this material was annealed at 160 C for 2 hours to reduce the ductility. After 2 hours of heat treatment, the fine microstructure had phases with a mean linear intercept length of 4.6 microns as seen in

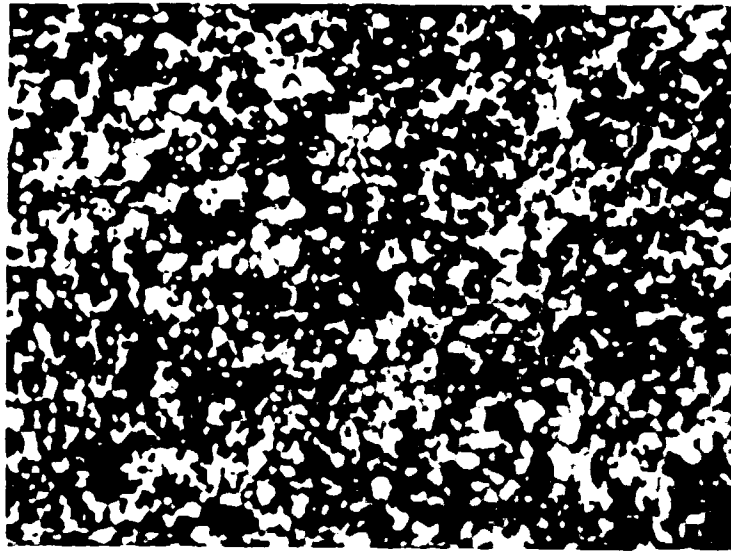


Figure 1: Microstructure of Lead-Tin as Cast (1000X)

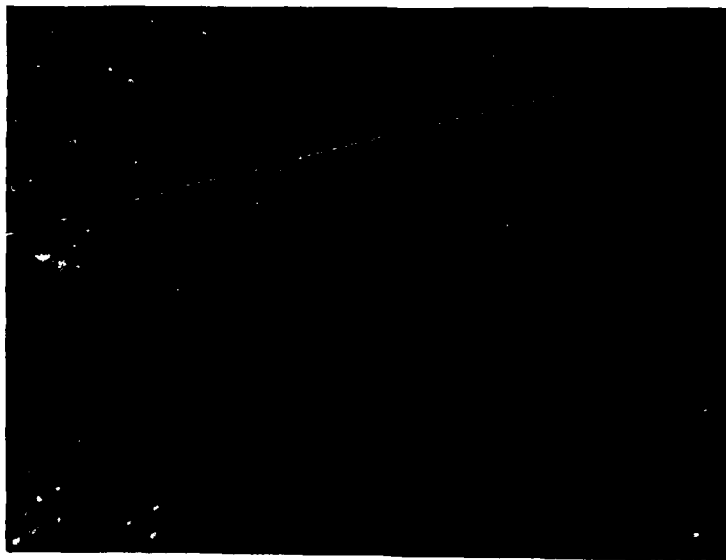


Figure 2: Microstructure of Lead-Tin 95% Reduction (1000X)

Figure 3. Annealing the cold rolled lead-tin did not change the grain size very much as seen in these micrographs.

Aluminum-Bronze

The aluminum-copper system has a eutectic point at 8.3 weight percent aluminum and a eutectoid point at 11.8 weight percent aluminum. Figure 4 shows the binary phase diagram for the copper rich end of the aluminum-copper system (6). An aluminum-bronze alloy of Cu-10-11%Al-3-5% Fe was purchased from Ampco Metals Company in the form of a 1 inch thick by 3 inch wide continuously cast bar. Figure 5 shows the as-received microstructure which consisted of a mixture of primary grains in a eutectoid matrix. This aluminum-bronze was hot rolled at 1700 F (925°C) to a final thickness of 0.050 inch with a reduction in thickness of 0.025 inch per pass. After rolling, the aluminum-bronze was annealed at 800°C for 1/2 hour and allowed to air cool.

Figure 6 shows the final microstructure. After hot rolling and annealing, the structure consisted of grains, which had been broken up into a smaller size of 1 to 2 microns, in a eutectoid matrix. This rolled and annealed aluminum-bronze is slightly ductile at room temperature but could be more easily formed at temperatures near 800°C where it is more ductile. A total of 976 square inches of the annealed aluminum-bronze was delivered.



Figure 3: Microstructure of Lead-Tin 95%
Reduction and Heat Treated
2 hours at 160°C (500X)

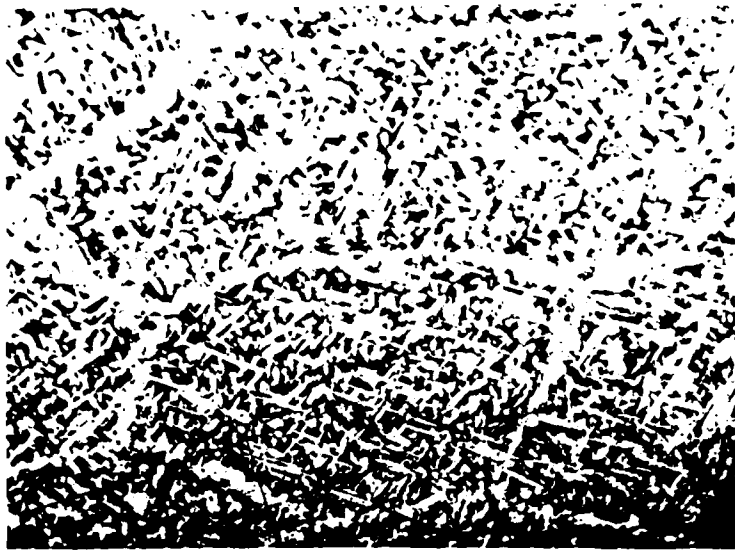


Figure 5: Microstructure of Aluminum-Bronze As-cast (100X)

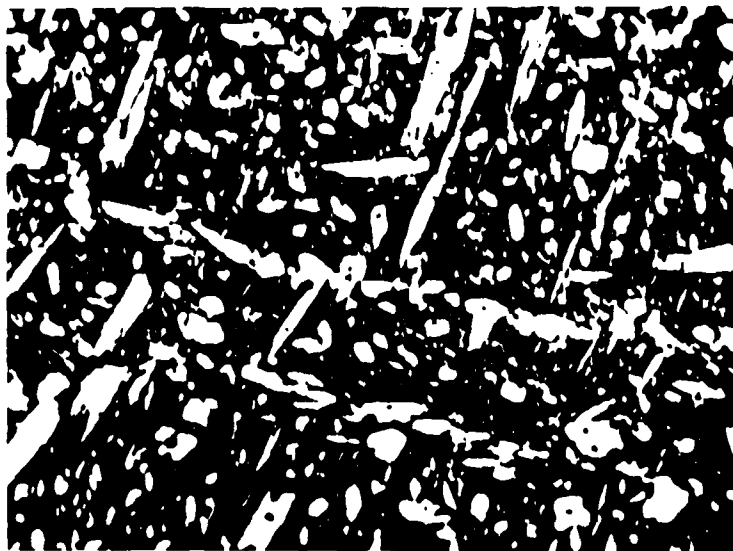


Figure 6: Microstructure of Aluminum-Bronze 95% Reduction and Annealed (500X)

Eutectic Lead-Antimony

Eutectic lead-antimony (11.2 weight percent antimony) was made by melting St. Joseph lead (99.9% pure) with pure antimony. This eutectic lead-antimony was cast into an iron mold which was coated with Aquadag. The cast ingots 1 inch thick by 3 inches wide were allowed to cool to room temperature in air. Figure 7 shows the microstructure of the as-cast lead-antimony. It shows that the as-cast structure consisted of a coarse lamellar structure consisting of a white antimony rich phase and a dark lead rich phase. Segregation during casting caused the formation of large dark dendrites of lead and white primary antimony crystals. The cast lead-antimony was heated at 135°C (275°F) and rolled to a 50 percent reduction.

It was rolled with a 0.050 inch reduction in thickness per pass on the rolling mill. After rolling to a 50 percent reduction, the casting was rolled to a final 94 percent reduction at room temperature. The final lead-antimony sheet was 0.065 inches thick. Figure 8 shows the lead-antimony rolled to a 94 percent reduction. The structure consisted of a fine microstructure with phases on the order of 1 to 2 microns. Cubic particles of primary antimony 10 to 20 microns in size were also present in the as-rolled lead-antimony. Rapid quenching of the molten lead-antimony should provide a more homogeneous structure than the cast alloy.

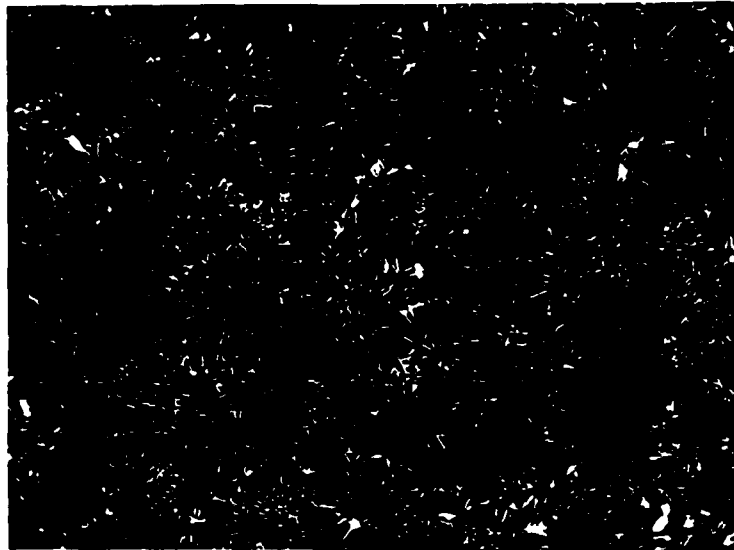


Figure 7: Microstructure of Lead-Antimony
As Cast (100X)



Figure 3: Microstructure of Lead-Antimony
94% Reduction (500X)

Eutectic lead-antimony was remelted and rapidly quenched in a water bath. The result of quenching in water was to form moss, which were thin flakes of lead-antimony about a half-inch in diameter. The moss was mounted and polished to show a uniform eutectic microstructure as in Figure 9. This microstructure was entirely eutectic with no primary lead or antimony segregation. Specimens were made from the moss by pressing at 10,000 psi, sintering at 200°C (390°F) and severe rolling to bond the particles. To further improve the processing technique, lead-antimony was crucible melt extracted. A 6 inch diameter copper disk with an 0.125 inch flat machined on the disk periphery was used for the crucible melt extraction process. The disk rotated at 700 rpm which gave a fiber production rate of close to 18.3 ft/s. Figure 10 shows the microstructure of the melt extracted fibers. It had a very uniform and homogeneous eutectic structure. An attempt was made to extrude the melt extracted fibers, but a layer of lead oxide prevented bonding. The 12 to 1 extrusion ratio used was not high enough to consolidate the fibers into a dense compact.

Crucible melt extracted fibers were remelted in a large plumbago crucible and allowed to air cool from the outside to the center. A stainless steel rod bent into an "S" shape was used to stir the melt as it cooled. Vigorous stirring of the melt should prevent segregation of the lead and antimony. After it was cold, the casting was band sawed into 1 inch thick sections so they could be rolled. The as-cast microstructure is shown in Figure 11. The stir cast lead-antimony consisted of a microstructure of

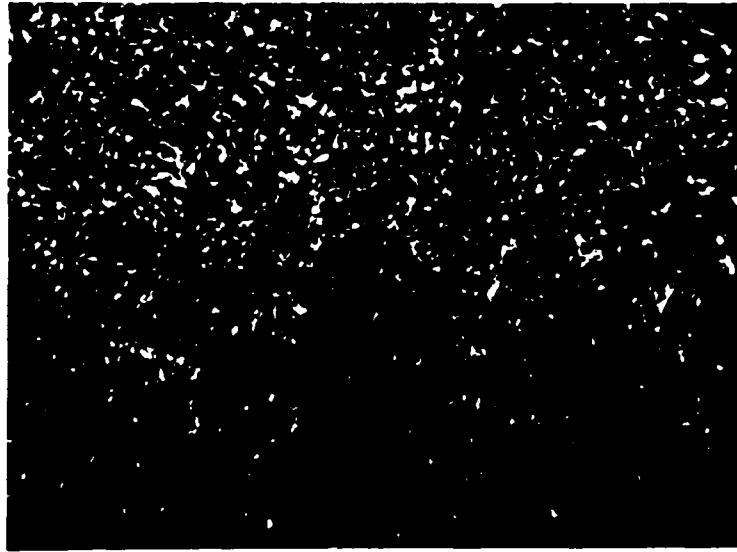


Figure 9: Microstructure of Lead-Antimony Moss (1000X)



Figure 10: Microstructure of Lead-Antimony Fibers (150X)

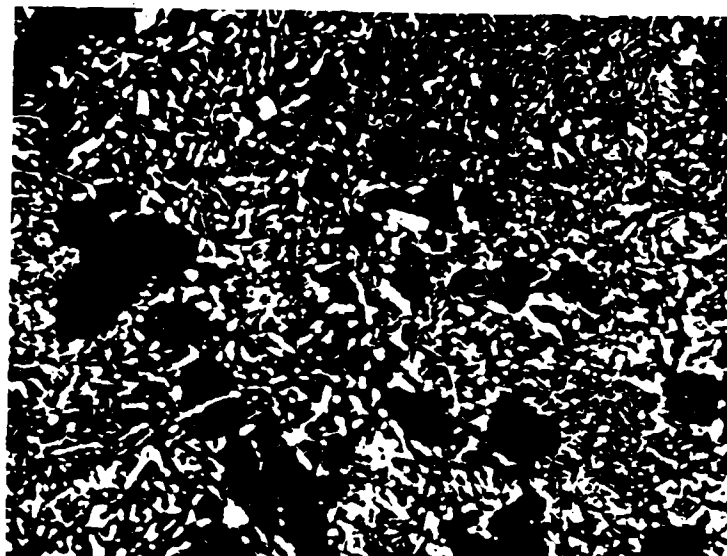


Figure 11: Microstructure of Lead-Antimony
Stir-Cast (100X)

primary lead dendrites, a few antimony crystals and a coarse eutectic phase.

The stir cast lead-antimony was heated to 200°C for 1/2 hour and hot rolled to a 50 percent reduction. After a 50 percent reduction, it was rolled at room temperature to a final reduction of 97 percent. Figure 12 shows the microstructure of the lead-antimony rolled to a 97 percent reduction. The final structure still had primary antimony crystals in a fine eutectic of lead rich solid solution and antimony rich solid solution. The large antimony crystals were about 80 microns in diameter while the small ones were 20 microns in diameter. A total of 882 square inches of the stir cast and rolled lead-antimony was delivered.

Tensile Testing of Superplastic Alloys

Tensile specimens were made from the rolled sheets of eutectic lead-tin with a 1 inch gauge length and a gauge width of 0.20 inch. The sheet tensile specimens were tested at crosshead speeds of 0.02 cm/min ($1.3 \times 10^{-4} \text{ sec}^{-1}$) and 0.2 cm/min ($1.3 \times 10^{-3} \text{ sec}^{-1}$) at room temperature. At a $1.3 \times 10^{-4} \text{ sec}^{-1}$ initial strain rate, an elongation of 644 percent was possible. Increasing the strain rate to $1.3 \times 10^{-3} \text{ sec}^{-1}$ caused the elongation to decrease to 394 percent. Cold rolling the lead-tin alloy was sufficient mechanical processing to refine the grain size and cause the lead-tin to be superplastic. Sheets of rolled tensile eutectic lead-tin were heat treated at 160°C (433°K) for 1 to 5 hours. The results of heat treated lead-tin are summarized in Table I.

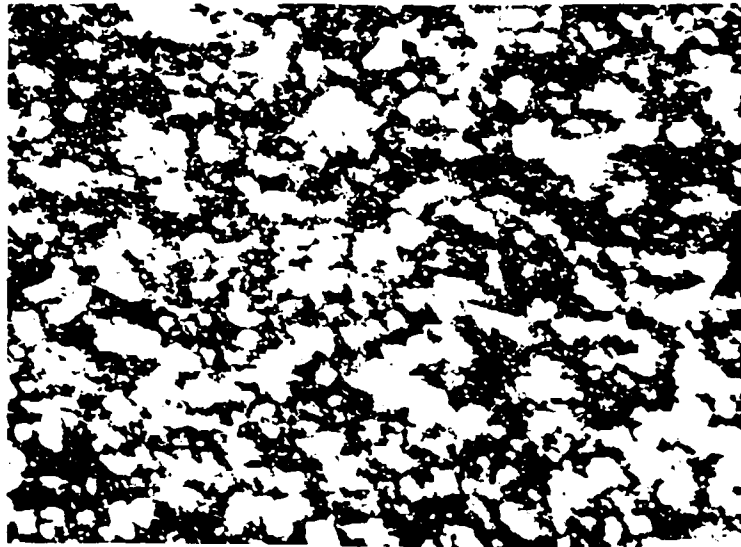


Figure 12: Microstructure of Lead-Antimony
97% Reduction (500X)

Table I. Heat Treatment of Lead-Tin

Time at 160°C (hours)	Mean Linear Longitudinal Intercept Length (microns)
0	3.6
1	4.2
2	4.6
3	5.1
4	5.0
5	5.4

These results showed that heat treating the alloy at 160°C did not appreciably change the grain size. Figure 13 shows that the elongation dropped from 175 to 44 percent after 5 hours at 160°C. To investigate the effect of heat treating at the lower temperatures of 120°C, 80°C, and room temperature, the microhardness was measured with time after rolling. Figure 14 shows that the Vickers microhardness tended to level out after only 2 hours of heat treating. At room temperature the hardness leveled out after only 24 hours as seen in Figure 15. These results showed that the as-rolled structure in the lead-tin was not stable at room temperature and the elongation dropped with time.

The sheets of eutectic lead-tin were heat treated for 2 hours at 160°C to remove the as-rolled structure. When the heat treated sheets were tensile tested, they had an elongation of 181 percent compared to an elongation of 394 percent for the freshly rolled material tested at $1.3 \times 10^{-3} \text{ sec}^{-1}$.

Tensile tests were conducted on samples of rolled and annealed aluminum-bronze at room temperature. The longitudinal tensile specimens had an ultimate tensile strength of 89,745 psi when they were tested at a strain rate of $1.3 \times 10^{-4} \text{ sec}^{-1}$. 12.5 percent elongation was measured for the aluminum-bronze.

Transverse tensile specimens had a tensile strength of 87,760 psi and a 6.3 percent elongation. Such a low value for the elongation made deformation at room temperature almost impossible. Previous results by Dunlop et al. showed that a

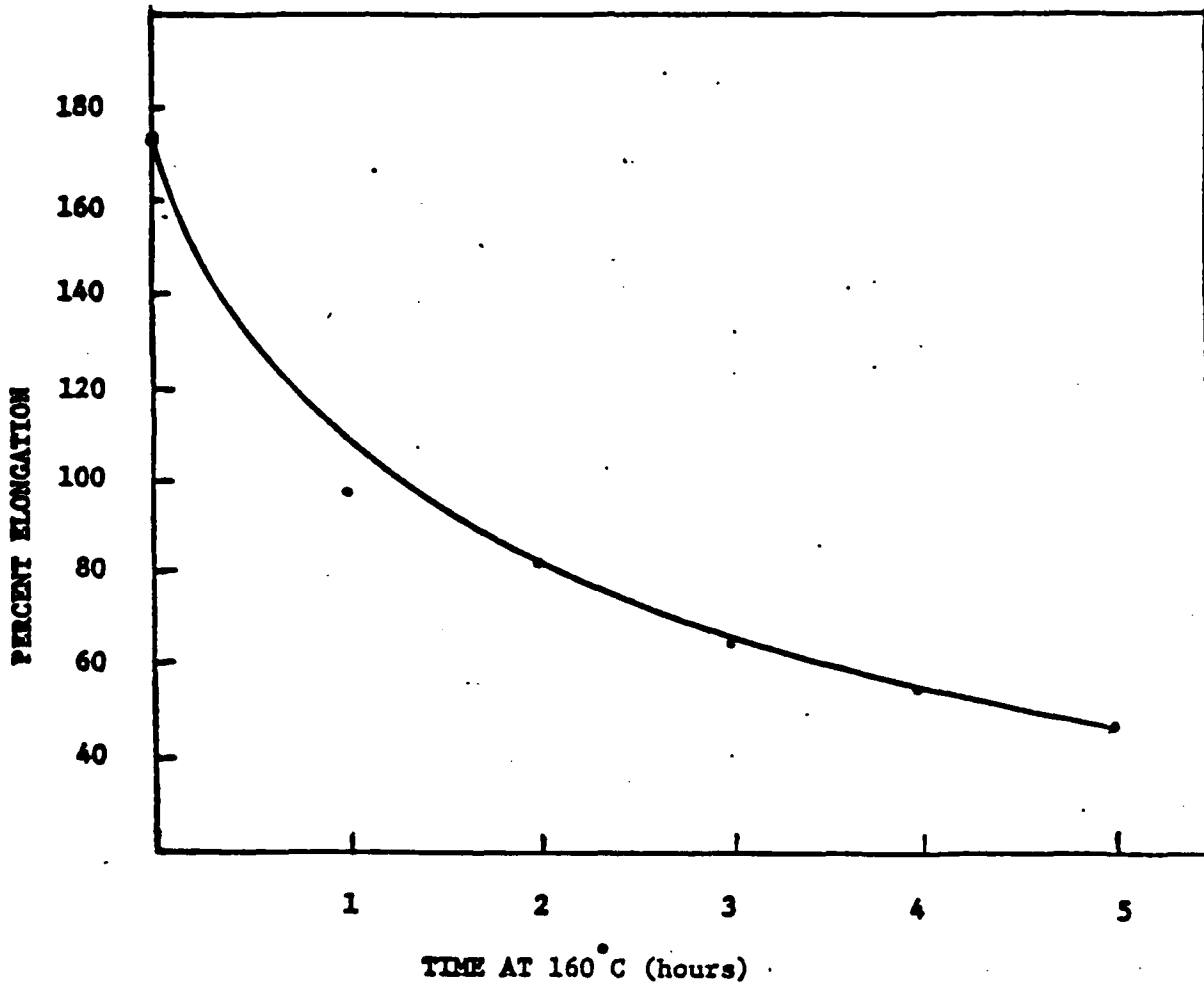
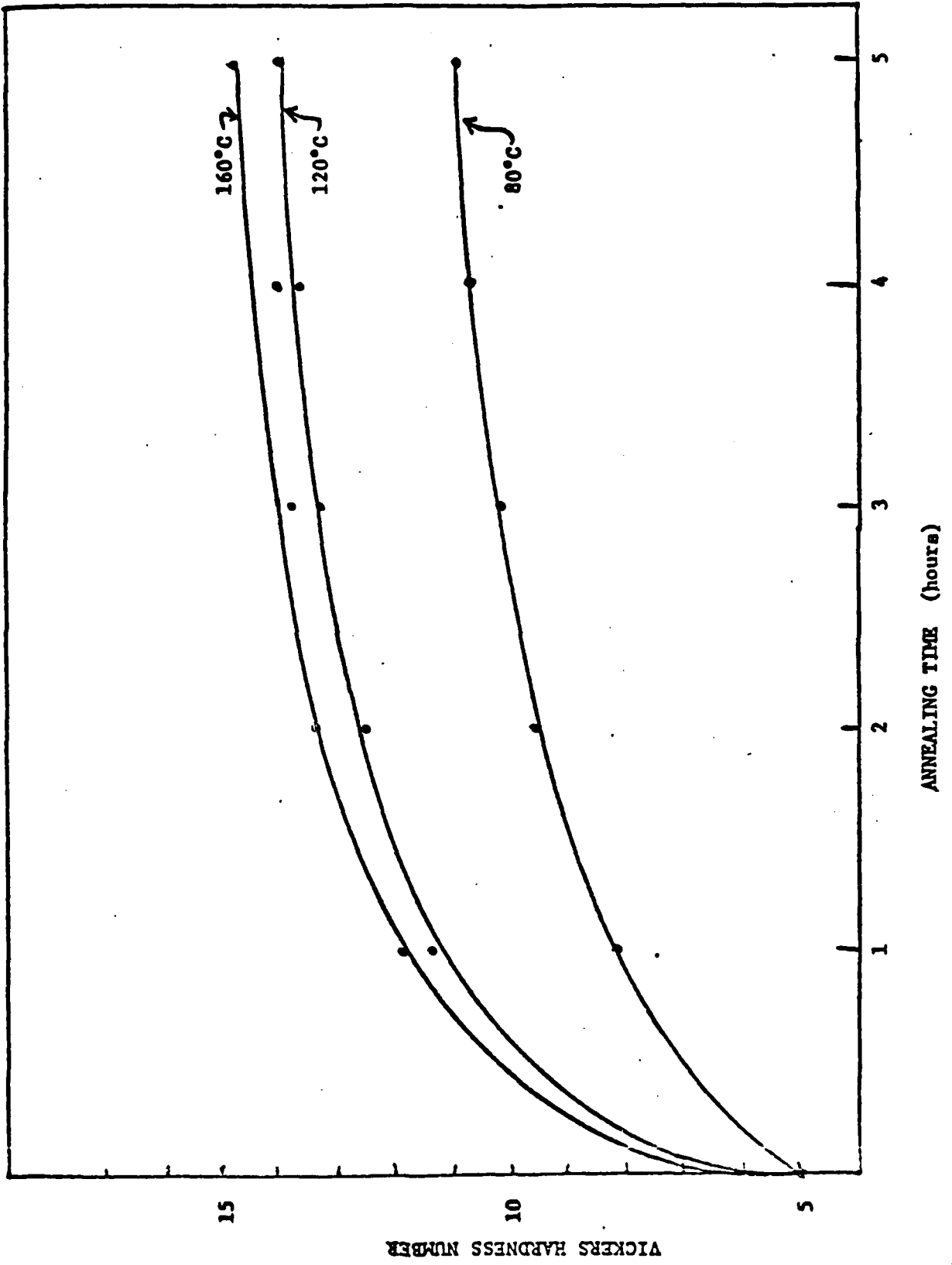


Figure 13: Elongation versus Annealing Time for Eutectic Lead-Tin



VICKERS HARDNESS NUMBER

ANNEALING TIME (hours)

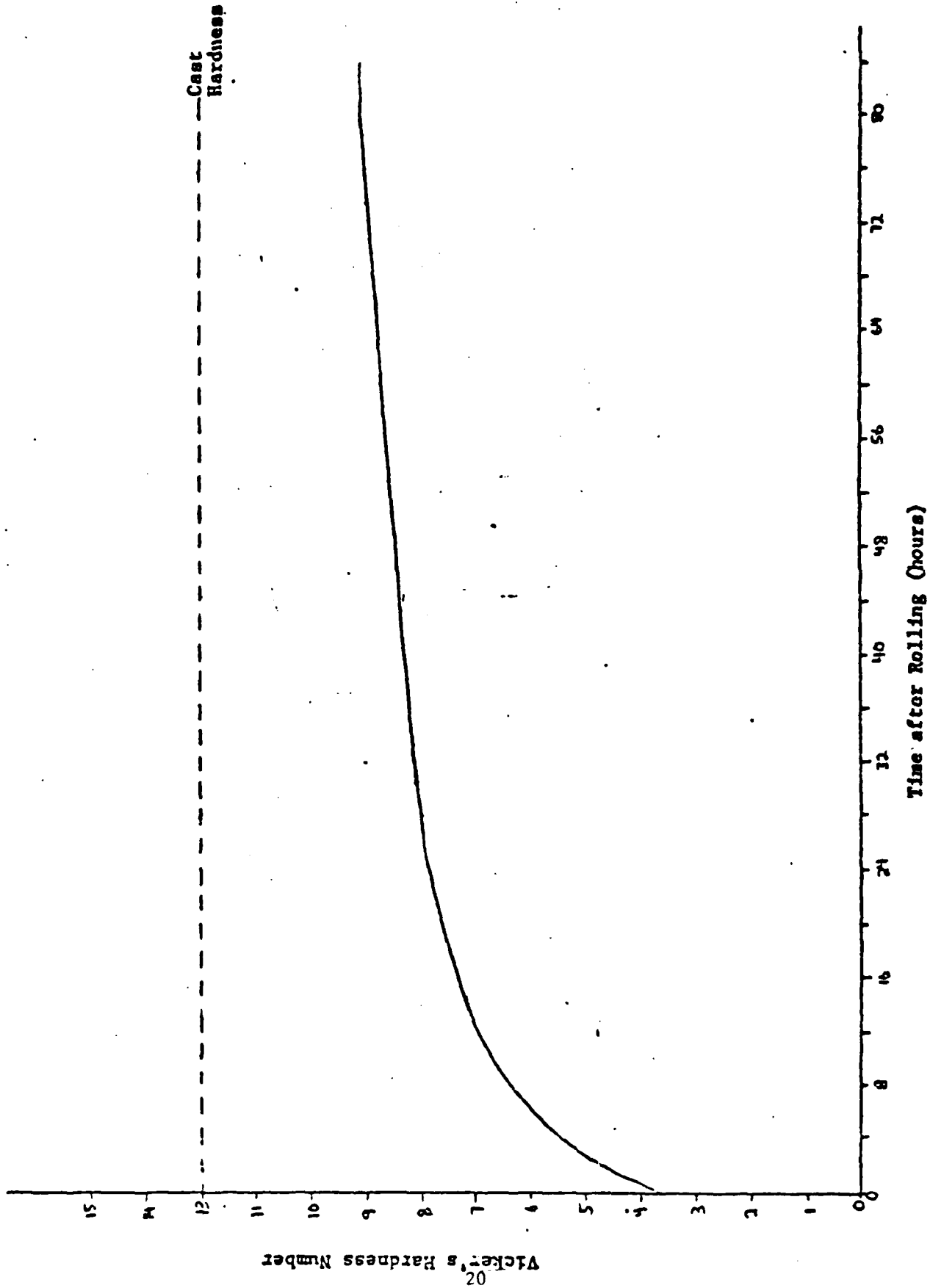


Figure 15: Hardness versus Annealing Time at Room Temperature for Lead-Tin

similar aluminum bronze had an elongation of over 700 percent when it was tested at 800°C (7).

Eutectic lead antimony tensile tests at $1.3 \times 10^{-4} \text{ sec}^{-1}$ showed a dramatic change in values as the structure was made more homogeneous as seen in Table II.

Alloying the eutectic lead-antimony with tin to form the 80 Pb-10Sb-10Sn pseudobinary eutectic alloy caused the elongation to increase from a low value of 40 percent to 144 percent. There were few cubic antimony crystals in the structure, but 5-10 micron size SbSn intermetallic particles were present.

Zinc and Zinc Alloys

Results

The angular dispersive x-ray traces were obtained by using a Diano CA7 copper medium focus x-ray tube on a General Electric SPG Goniometer and a XRD-5 Diffraction Unit. A flat rolled sheet is rotated by θ degrees while the x-ray detector is rotated through 2θ degrees. The x-ray detector is scanned through increasing values of 2θ while the x-ray intensity is measured. A 3 degree medium resolution incident beam slit and a 0.2 degree divergence beam slit was chosen for the x-ray diffraction results. A General Electric No. 2 SPG Detector proportional counter was scanned at 4 degrees per minute to obtain the angular dispersive spectra. The copper $K\beta$ radiation was filtered out of the results by a nickel filter placed in front of the x-ray detector. These parameters are summarized in Table III.

Table II. Elongation of Lead-Antimony Alloys at Room Temperature

Material	Percent Elongation
Lead-Antimony (Cast and Rolled)	40- 63 percent
Lead-Antimony (Stir cast and Rolled)	44 percent
Lead-Antimony Moss (Rapidly Solidified and Rolled)	68- 75 percent
Lead-Antimony Fibers (Extracted-Extruded-Rolled)	110 percent

Table III. Angular Dispersive Results for the Pure Zinc

Intensity for Pure Zinc at Angle (2θ),
(counts/sec.)

Percent Rolling Reduction	36.4 (0002)	39.0 (10 $\bar{1}$ 0)	43.5 (10 $\bar{1}$ 1)	54.5 (10 $\bar{1}$ 2)	70.2 (11 $\bar{2}$ 0)
25	800	750	800	540	450
50	900	950	>1000	630	620
75	700	660	>1000	560	730
90	460	450	>1000	660	600

Table IV. Angular Dispersive Results for the Zinc/Copper

Intensity for Zinc/Copper at Angle (2θ),
(counts/sec.)

Percent Rolling Reduction	36.4 (0002)	39.0 (10 $\bar{1}$ 0)	43.5 (10 $\bar{1}$ 1)	54.5 (10 $\bar{1}$ 2)	70.2 (11 $\bar{2}$ 0)
25	>1000	500	>1000	530	580
50	1500	750	2500	700	500
75	260	400	1600	600	500
90	500	450	2500	1000	600

Table V. Pure Zinc Diffractometer Measurements

Percent Rolling Reduction	(0002) 2θ Degrees	(10 $\bar{1}$ 0) 2θ Degrees	c	a	c/a
25	36.08	38.80	4.974 Å	2.677 Å	1.858
50	36.45	39.04	4.925 Å	2.662 Å	1.850
75	36.34	38.83	4.940 Å	2.675 Å	1.847
90	36.2	38.76	4.958 Å	2.680 Å	1.850
95	36.33	39.04	4.941 Å	2.662 Å	1.856
98	36.5	39.28	4.919 Å	2.646 Å	1.859

Table IV shows the angular dispersive analysis results for the zinc alloyed with 88 ppm. of copper. Both tables show a similar trend. The intensity due to the basal planes (0002) has decreased while the intensity of the (10 $\bar{1}$ 1) planes has increased in both cases. This change in intensity would indicate that the zinc and zinc-copper alloy tends to develop a preferred crystallographic orientation or texture as the material is rolled. Rolling the zinc did not significantly lower the x-ray intensities, but it did show that certain peaks decreased in intensity while the (10 $\bar{1}$ 1) peaks increased.

Lattice parameter calculations were made with the angular dispersive results. These values for the c/a ratio are shown in Table V. The c/a ratio decreases up to a 75 percent rolling reduction and then it increases back to a normal ratio of 1.859. These results suggest that the density should be at a maximum at a 75 or 90 percent rolling reduction.

X-ray Pole Figures

To investigate the development of a rolling texture in the case of the zinc, X-ray pole figures were analyzed. X-ray pole figures for the zinc and zinc-copper samples were obtained by using a CA8-L copper tube in a Siemens Texture Diffractometer. A nickel filter was used to remove the K β copper radiation from the diffracted radiation. The modified Siemens pole figure goniometer rotated the flat specimens 360 degrees and tilted the specimens from 0 to 90 degrees. This goniometer arrangement takes

data on the entire stereographic projection by tracing a continuous spiral from the outside of the projection to the center. Strip charts show the x-ray intensity at any position along the spiral on the stereographic projection. A texture free sample of sintered copper powder was used to normalize the measured intensities. This texture free sample should have one intensity value at every point on the stereographic projection and can be used to calibrate the intensity values.

To obtain a pole figure, the x-ray detector is set at the 2θ which will satisfy the Bragg law for a given type of crystalline planes. From Bragg's Law, $n\lambda = 2d \sin\theta$, the exact angle can be chosen for diffraction. The wave length, λ , of the copper radiation and the planar spacing of zinc, d , are known. The diffracting angle 2θ can be set and the sample rotated so all possible lattice orientations have a chance to satisfy these diffraction conditions.

Pure zinc and the zinc/copper alloy were rolled to reduction of 25, 50, 75, 90, 95, and 98 percent and pole figures for the (0002) and (10 $\bar{1}$ 1) planes were drawn. After a 75 percent rolling reduction, a texture develops in which the basal plane (0002) is tilted 30-40 degrees toward the rolling direction. In the zinc with 88 ppm. copper, a strong rolling texture develops after a 50 percent reduction and remains up to a 98 percent reduction. The texture in the alloy appears to be the same as the rolling texture in the pure zinc.

The pole figure traces show an increased background intensity as the zinc is rolled with identical instrument settings. To measure the change in the background as a function of rolling, the area under the pole figure was integrated for the (10 $\bar{1}1$) pole figure traces. Table VI shows the data for the areas under the pole figure trace for the pure zinc. The areas under the crystalline peaks were measured first and then the area under the background radiation was measured. The peak area to total area ratio was calculated by dividing the crystalline peak area by the sum of the crystalline peak area and the background area. This value can be visualized as a measure of the volume percent of crystalline material to the volume percent of disordered or amorphous material.

At a reduction of 75 percent, there is a drop in the value of the crystalline peak area to the total area. The value increases at a 90 percent reduction to 18.2 percent since the background level has decreased to a low value. The percent peak area to total area decreases with further rolling to a 98 percent reduction. You should notice that the increase in background area accounts for this noticeable decrease. These values indicate that the structure is becoming less crystalline and more disordered with rolling since the planes are no longer aligned to cause diffraction. At a 98 percent rolling reduction, the crystalline peak area to the total area is only 13.2 percent. After two months, the area under the peaks has increased which would indicate that crystallization has occurred. The values for the areas under the background have not changed very much. The

Table VI. Values of the Integrated Areas
Under the (10 $\bar{1}1$) Pole Figure Trace
for Pure Zinc (99.999 Percent Pure)

Percent Reduction by Rolling	Area Under the Peaks (in ²)	Area Under the Background (in ²)	Peak Area (100) Total Area
25	41.1	141.6	22.5
50	30.8	65.9	31.8
75	26.0	188.6	12.1
90	25.5	114.7	18.2
95	27.7	165.6	14.3
98	27.4	180.0	13.2
TWO MONTHS LATER			
25	59.4	142.3	29.4
50	56.5	149.1	27.5
75	52.3	206.1	20.2
90	47.0	133.5	26.0
95	55.2	167.0	24.8
98	60.3	203.9	22.8

jump in the crystalline peak area to the total area at 90 percent reduction may be explained by the material re-crystallizing at room temperature during the rolling process. As the rolling process continues above a 90 percent reduction, the material is becoming more disordered again as it is rolled.

The values of the integrated areas under the pole figure for zinc with 88 ppm. of copper are shown in Table VII.

The data shows that the area under the crystalline peaks is continuously decreasing with rolling down to a 98 percent reduction. The crystalline peak area to the total area under the pole figure trace also decreases as the material is rolled. These x-ray results were obtained by looking at the $(10\bar{1}1)$ planes which had the most intense peaks in the angular dispersive x-ray results. The zinc with copper sample did not re-crystallize when it was rolled.

The values for the percent crystalline peak area divided by the total area are shown again in Figures 16 and 17.

Density Measurements

Densities were measured for the samples of pure zinc and zinc with 88 ppm. of copper. These were made by using Archimedes Method for determining densities. The variation in density with rolling is shown in Figure 18. After heat treating at 350°C and air cooling, the density of the pure zinc was 7.1523 gms/cm³. The zinc recrystallized after a 90 percent reduction

Table VII. Values of the Integrated Areas Under the (1011) Pole Figure Trace for Zinc/Copper

Percent Reduction by Rolling	Area Under the Peaks (in ²)	Area Under the Background (in ²)	$\frac{\text{Peak Area (100)}}{\text{Total Area}}$
25	124.7	246.1	33.6
50	129.1	266.7	32.6
75	93.6	228.4	29.1
90	71.2	225.4	24.0
95	73.9	212.5	25.8
98	69.6	216.2	24.3

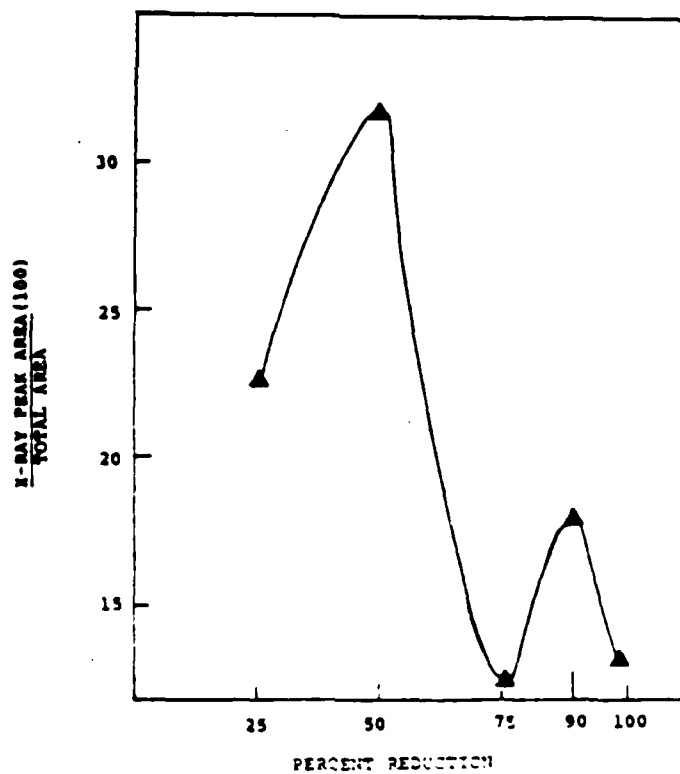


Figure 16: Variation in the X-Ray Peak Area Divided by Total Area versus Percent Reduction for Pure Zinc

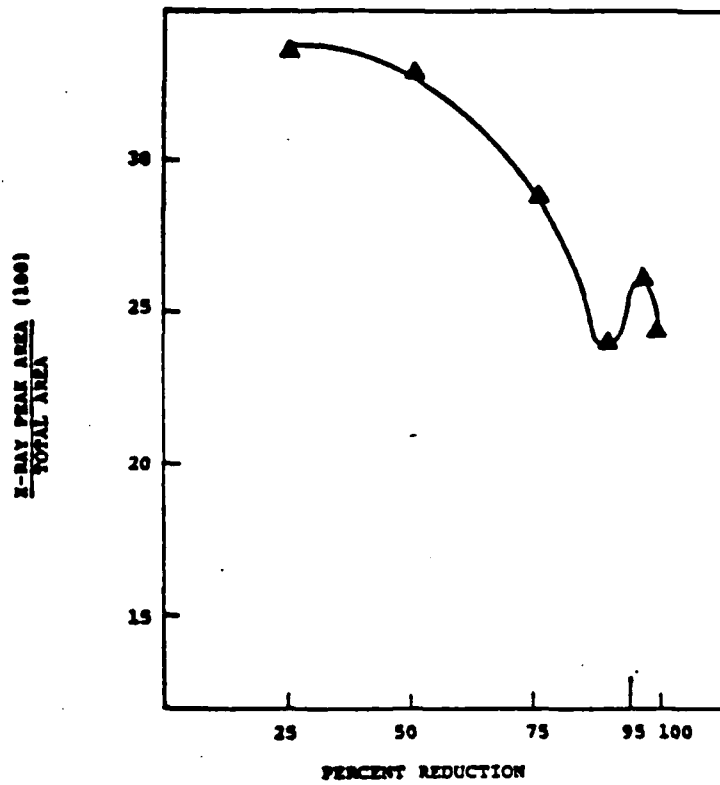


Figure 17: Variation in the X-Ray Peak Area Divided by Total Area versus Percent Reduction for Zinc with 88 ppm. Copper

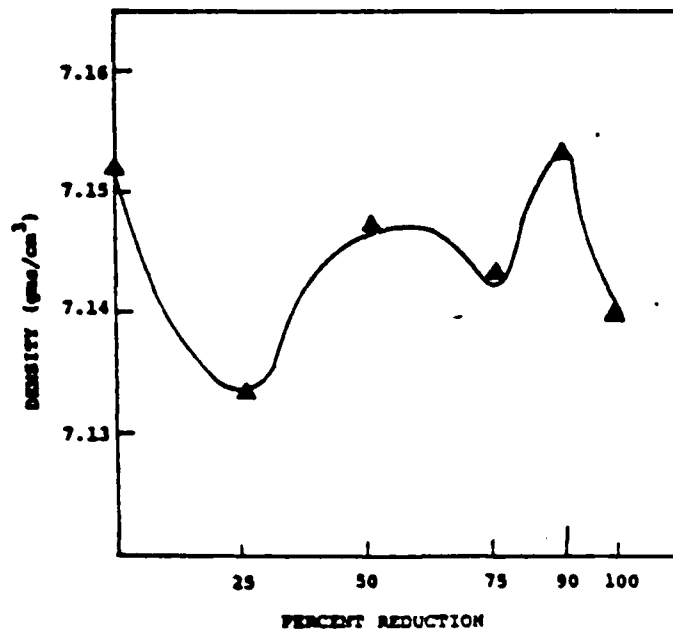


Figure 18: Variation in Density with cold rolling Pure Zinc

because there is a peak in the density. Further rolling caused the density to decrease. Figure 19 shows the variation in density with rolling for the zinc with 88 ppm. of copper. The original heat treated and air cooled density was 7.1528gms/cm and this density decreased to a 90 percent reduction.

Relaxation occurred at a 95 percent reduction with a peak in the density curve. Further cold rolling caused the density to drop again. In summary, the pure zinc underwent relaxation at a 90 percent reduction whereas the zinc with copper relaxed after a 95 percent reduction. The figures for the x-ray percent crystalline material agree very well with the curves for the density.

Microhardness profiles were obtained for the two zinc samples using a Leco M400 microhardness tester with a 10 gram load and a 2 second load time. Figure 20 shows the Vickers hardness number as a function of distance from the grain boundary for the pure zinc. There was a soft region about 10 microns wide on either side of the grain boundary. In Figure 21, the microhardness profile for the zinc with 88 ppm. of copper showed a soft region that extended approximately 50 microns on either side of the grain boundary. Cold rolling the pure zinc caused both the boundary hardness and grain hardness to decrease as seen in Figure 22.

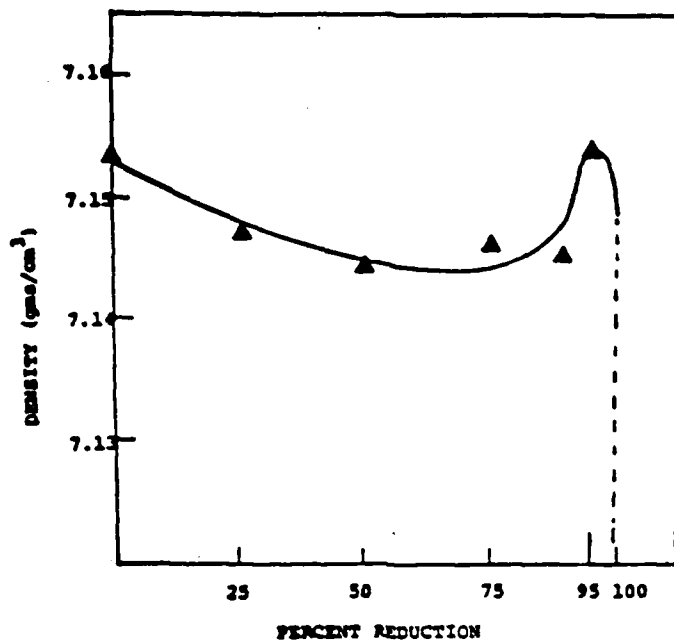


Figure 19: Variation in Density with Cold Rolling Zinc-88 ppm. Copper

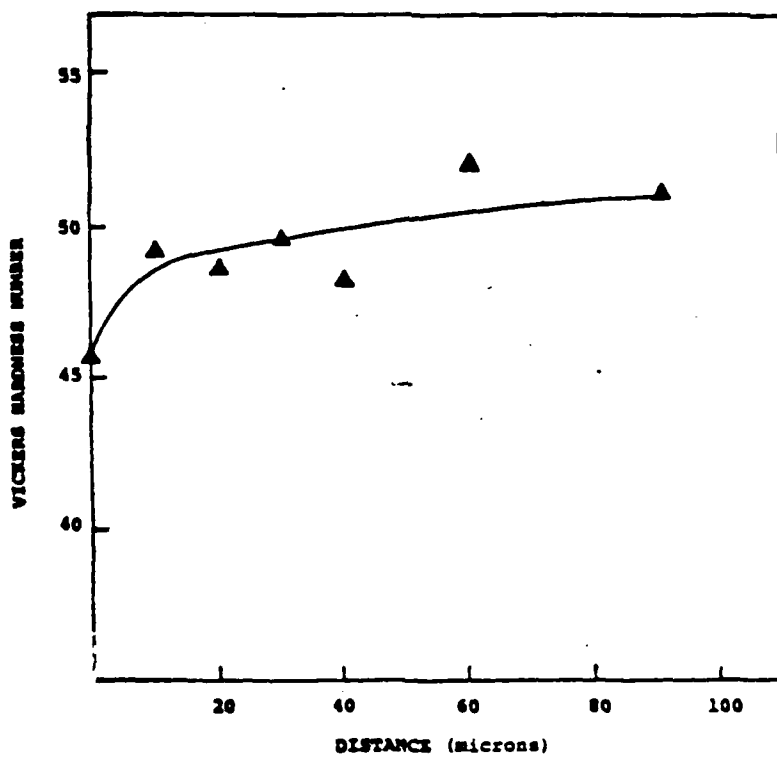


Figure 20: Hardness-Distance Profile Pure Zinc

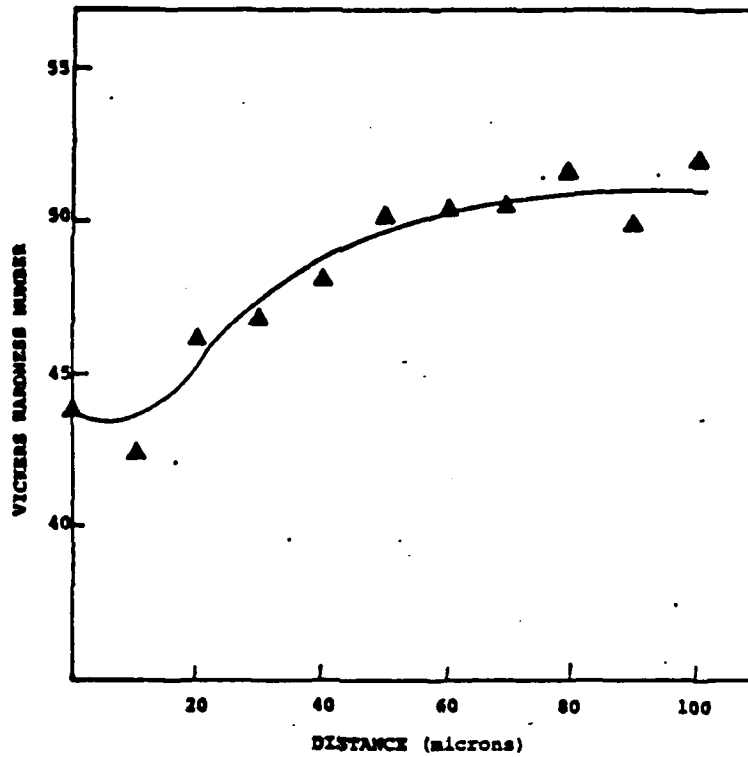


Figure 21: Hardness-Distance Profile
Zinc-88 ppm. Copper

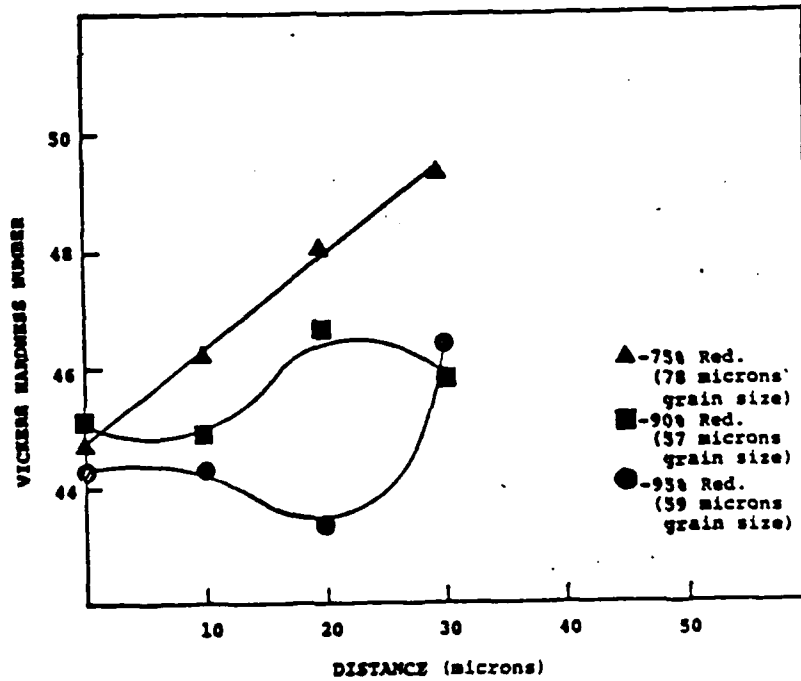


Figure 22: Hardness-Distance Profile
After Cold Rolling Pure Zinc

After rolling to a 90 percent reduction, the soft region extended out to 20 microns from the boundary. This soft 20 micron region was a large portion of the volume when the grain size was 57 microns. In the zinc with copper, the grain boundary region was about 20 microns wide as seen in Figure 23. The average grain size had decreased to 42 microns after a 90 percent reduction. Most of the volume was the soft material near the grain boundary. Such a large volume of ductile material would enhance the grain boundary sliding at slow strain rates.

Summary

1. Eutectic lead-tin, eutectic lead-antimony, and aluminum bronze were thermomechanically processed to enhance their room temperature ductility. Cold rolling enhanced the ductility of the lead-tin and lead-antimony. The ductility of the aluminum-bronze was not greatly affected by the hot rolling.
2. The ductility of the rolled lead-tin was shown to change with time when it was stored at room temperature.
3. Different processing procedures were used to obtain homogeneous lead-antimony eutectic. Compacting melt extracted fibers gave the most homogeneous structure and the best tensile results but proved to be difficult to apply on a larger production scale.
4. Microhardness results for both the pure zinc and zinc with 88 ppm. copper showed the existence of a soft grain boundary

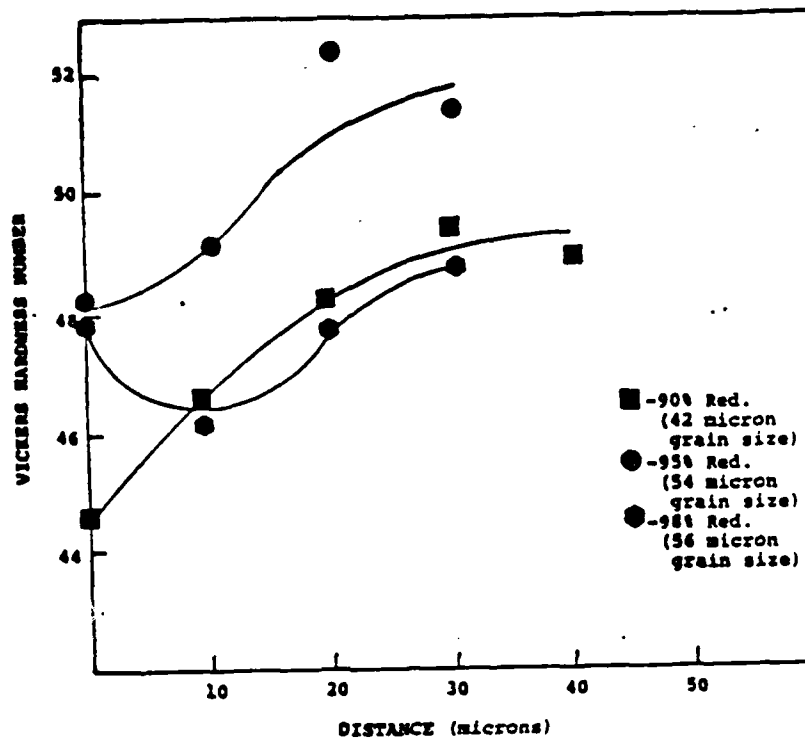


Figure 23: Hardness-Distance Profile
After Cold Rolling Zinc-88
ppm. Copper

region which is 20 microns wide on either side of the grain boundary after a 90 percent reduction in thickness.

This high entropy material accounted for a large volume of the grains since the grain size was only 50 microns.

5. The x-ray texture studies on the rolling of pure zinc indicated that a strong rolling texture developed and that it was necessary to integrate the areas under the texture spectrum. The peak area ratio to total area ratio was calculated by dividing the area under the peaks above the background level by the total area. This value can be visualized as a relative measure of the volume percent of perfect crystalline material to the total volume. These values showed that the pure zinc underwent relaxation after a 90 percent reduction. In the zinc with copper, the relaxation occurred after a 95 percent reduction in thickness. From these results it seems that the ductility enhancement was due to the presence of the highly disordered material within the polycrystalline mass. This metastable grain boundary material was required for the enhanced ductility and with time the material underwent relaxation to a more crystalline structure.

Recommendations for Future Work

The zinc experiments reported on suggest that a more room temperature stable metal should be used to verify the wide, soft grain boundary regions in the ductility enhanced material. With such a stable material the boundary structure and its relaxation with time and temperature can be determined. The selection of such a candidate material will be difficult but the work of Shei and Langdon (8) indicates that the copper base alloy Coronze CDA 638 becomes superplastic with proper thermo-mechanical treatment. The difficulty with using this alloy is that although primarily single phase, it is a quaternary.

It is recommended that future work consist of using pure copper as the candidate material and carrying out a program to find which single element micro-alloy addition will render the material superplastic with the appropriate thermo-mechanical treatment. Once a good system is selected then the grain boundary affected volumes should be studied by SEM and X-ray to establish their structure and stability.

References

1. C.E. Pearson: J. Inst. Metals, 1934, Vol. 54, p. 111.
2. Mohamed M.I. Ahmed and T.G. Langdon: Met. Trans. A., 1977, Vol. 8A, p. 1832.
3. H. Naziri and R. Pearce: J. Inst. Metals, 1969, Vol. 97, p. 326.
4. K.T. Aust, R.E. Hanneman, P. Niessen and J.H. Westbrook, Acta Met., Vol. 16, 1968, p. 291.
5. Angela Rosasco: Ph.D. Thesis "Structural Homogeneity, Crystallization and Embrittlement Behavior of $Fe_{81}B_{13.5}Si_{3.5}C_2$ ", The Johns Hopkins University, 1983.
6. ASM Metals Handbook, 1948 Edition, p. 1160.
7. G.L. Dunlop, J.D. Reid and D.M.R. Taplin: Met Trans., Vol. 2, Aug. 1971, p. 2308.
8. Shen-Ann Shei and T. G. Langdon: Acta Met., Vol. 26, 1978, p. 639.

DISTRIBUTION LIST

<u>No. of Copies</u>	<u>Organization</u>	<u>No. of Copies</u>	<u>Organization</u>
12	Administrator Defense Technical Info Center ATTN: DTIC-FDAC Cameron Station, Bldg 5 Alexandria, VA 22304-6145	1	Commander US Army Armament Research, Development and Engineering Center ATTN: SMCAR-MSI Dover, NJ 07801-5001
1	Deputy Assistant Secretary of the Army (R&D) Department of the Army Washington, DC 20310	1	Commander US AMCCOM ARDEC CCAC Benet Weapons Laboratory ATTN: Dr. E. Schneider Watervliet, NY 12189-4050
1	HQDA DAMA-ARP-P, Dr. Watson Washington, DC 20310	1	Director US AMCCOM ARDEC CCAC Benet Weapons Laboratory ATTN: SMCAR-CCB-TL Watervliet, NY 12189-4050
1	HQDA DAMA-ART-M Washington, DC 20310	1	Commander US Army Armament, Munitions and Chemical Command ATTN: AMSMC-IMP-L Rock Island, IL 61299-7300
1	HQDA DAMA-MS Washington, DC 20310	1	Commander US Army Aviation Systems Command ATTN: AMSAV-ES 4300 Goodfellow Boulevard St. Louis, MO 63120-1798
1	Commander US Army War College ATTN: Lib Carlisle Barracks, PA 17013	1	Director US Army Aviation Research and Technology Activity Ames Research Center Moffett Field, CA 94035-1099
1	Commander US Army Command and General Staff College ATTN: Archives Fort Leavenworth, KS 66027	1	Commander US Army Communications - Electronics Command ATTN: AMSEL-ED Fort Monmouth, NJ 07703-5301
1	Commander US Army Materiel Command ATTN: AMCDRA-ST 5001 Eisenhower Avenue Alexandria, VA 22333-0001		
1	Commander US Army ARDEC ATTN: SMCAR-TDC Dover, NJ 07801-5001		

DISTRIBUTION LIST

<u>No. of Copies</u>	<u>Organization</u>	<u>No. of Copies</u>	<u>Organization</u>
1	Commander US Army Communications- Electronics Command (CECOM) CECOM R&D Technical Library ATTN: AMSEL-IM-L B, 2700 Fort Monmouth, NJ 07703-5000	1	Commander US Army Natick Research and Development Center ATTN: DRXRE, Dr. D. Sieling Natick, MA 01762
1	Commander Harry Diamond Laboratories ATTN: DELHD-TA-L 2800 Powder Mill Road Adelphi, MD 20783	1	Commander US Army Tank Automotive Command ATTN: AMSTA-TSL Warren, MI 48397-5000
1	Commander US Army Missile Command Research, Development and Engineering Center ATTN: AMSMI-RD Redstone Arsenal, AL 35898	1	Commander USAG ATTN: Tech Lib Fort Huachuca, AZ 85613-6000
1	Director US Army Missile and Space Intelligence Center ATTN: AIAMS-YDL Redstone Arsenal, AL 35898-5500	1	Director US Army Advanced BMD Technology Center ATTN: CRDABH-5, W. Loomis P. O. Box 1500, West Station Huntsville, AL 35807
3	Director BMD Advanced Technology Center ATTN: ATC-T, M. Capps ATC-M, S. Brockway ATC-RN, P. Boyd P.O. Box 1500 Huntsville, AL 35807	1	Commander US Army Materials Technology Laboratory ATTN: SLCMT-H, S. C. Chou Watertown, MA 02172-0001
1	Director US Army Ballistic Missile Defense Systems Office 1320 Wilson Boulevard Arlington, VA 22209	1	Commander US Army Research Office ATTN: Dr. R. Weigle P. O. Box 12211 Research Triangle Park, NC 27709
2	Commander US Army Mobility Equipment Research & Development Command ATTN: DRDME-WC DRSME-RZT Fort Belvoir, VA 22060	1	Commander US Army Development and Employment Agency ATTN: MODE-ORO Fort Lewis, WA 98433-5000

DISTRIBUTION LIST

<u>No. of Copies</u>	<u>Organization</u>	<u>No. of Copies</u>	<u>Organization</u>
1	Director US Army TRADOC Analysis Center ATTN: ATOR-TSL White Sands Missile Range NM 88002-5502	1	AFWL/SUL Kirtland AFB, NM 87117
1	Commandant US Army Infantry School ATTN: ATSH-CD-CS-OR Fort Benning, GA 31905-5400	1	AUL (3T-AUL-60-118) Maxwell AFB, AL 36112
1	Office of Naval Research Department of the Navy ATTN: Code 402 Washington, DC 20360	1	AFFDL/FB, Dr. J. Halpin Wright-Patterson AFB, OH 45433
1	Commander Naval Surface Weapons Center ATTN: Code Gr-9, Dr. W. Soper Dahlgren, VA 22448	10	C.I.A. OIR/DB/Standard GE-47 HQ Washington, DC 20505
5	Commander US Naval Research Laboratory ATTN: C. Sanday R. J. Weimer Code 5270, F. MacDonald Code 2020, Tech Lib Code 7786, J. Baker Washington, DC 20375	5	Sandia National Laboratories ATTN: Dr. L. Davison Dr. P. Chen Dr. W. Herrmann Dr. C. Harness H.J. Sutherland P. O. Box 5800 Albuquerque, NM 87185-5800
1	AFATL (DLDG) Eglin AFB, FL 32542-5000		<u>Aberdeen Proving Ground</u>
1	AFATL/DOIL (Tech Info Center) Eglin AFB, FL 32542-5438		Dir, USAMSAA ATTN: AMXSY-D AMXSY-MP, H. Cohen
1	AFATL (DLYW) Eglin AFB, FL 32542		Cdr, USATECOM ATTN: AMSTE-SI-F Cdr, CRDC, AMCCOM ATTN: SMCCR-RSP-A SMCCR-MU SMCCR-SPS-IL
1	RADC (EMTLD, Lib) Griffiss AFB, NY 13440		

USER EVALUATION SHEET/CHANGE OF ADDRESS

This Laboratory undertakes a continuing effort to improve the quality of the reports it publishes. Your comments/answers to the items/questions below will aid us in our efforts.

1. BRL Report Number _____ Date of Report _____

2. Date Report Received _____

3. Does this report satisfy a need? (Comment on purpose, related project, or other area of interest for which the report will be used.) _____

4. How specifically, is the report being used? (Information source, design data, procedure, source of ideas, etc.) _____

5. Has the information in this report led to any quantitative savings as far as man-hours or dollars saved, operating costs avoided or efficiencies achieved, etc? If so, please elaborate. _____

6. General Comments. What do you think should be changed to improve future reports? (Indicate changes to organization, technical content, format, etc.) _____

CURRENT
ADDRESS

Name

Organization

Address

City, State, Zip

7. If indicating a Change of Address or Address Correction, please provide the New or Correct Address in Block 6 above and the Old or Incorrect address below.

OLD
ADDRESS

Name

Organization

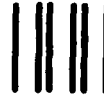
Address

City, State, Zip

(Remove this sheet, fold as indicated, staple or tape closed, and mail.)

FOLD HERE

Director
US Army Ballistic Research Laboratory
ATTN: DRXBR-OD-ST
Aberdeen Proving Ground, MD 21005-5066



NO POSTAGE
NECESSARY
IF MAILED
IN THE
UNITED STATES

OFFICIAL BUSINESS
PENALTY FOR PRIVATE USE, \$300

BUSINESS REPLY MAIL
FIRST CLASS PERMIT NO 12062 WASHINGTON, DC
POSTAGE WILL BE PAID BY DEPARTMENT OF THE ARMY



Director
US Army Ballistic Research Laboratory
ATTN: DRXBR-OD-ST
Aberdeen Proving Ground, MD 21005-9989

FOLD HERE

END

10-87

DTIC